Performances of Order Statistics CFAR

MORDECHAI SHOR

NADAV LEVANON, Senior Member, IEEE
Tel-Aviv University

Previous analysis of order statistics constant false-alarm rate (OS-CFAR) receiving a single pulse from a Rayleigh fluctuating target in a Rayleigh background is extended to a Rayleigh-plus-dominant target. The analysis includes effects of a multitarget environment.

Detailed comparison between OS-CFAR, CA-CFAR, and censored CA-CFAR, is provided for a Rayleigh target in the presence of strong interfering targets.

The false alarm analysis of OS-CFAR is extended to the more general case of a Weibull background. This allowed evaluation of the deterioration of the CFAR property of OS as the shape factor, C, of a Weibull probability density function (pdf) changes from Rayleigh ($C = 2$) to a longer tailed one ($C < 2$).

All the results for a single pulse detection appear as explicit analytic expressions. Integration of N pulses is also studied, for a Swerling II target. The OS-CFAR performances for that case yielded an integral equation which is evaluated numerically.

Manuscript received January 10, 1989; revised July 10, 1989.

IEEE Log No. 41902.

Authors' current addresses: M. Shor, Motorola, Israel; N. Levanon, Dep't. of Electronic Systems, Tel-Aviv University, P.O. Box 39040, Ramat Aviv, Tel-Aviv, 69978, Israel.

0018-9251/91/0300-0214 $1.00 © 1991 IEEE

I. INTRODUCTION

Order statistics (OS) CFAR [1], is a constant false alarm rate technique which is relatively immune to the presence of interfering targets among the reference cells. In a previous analysis [2] the performances of OS CFAR for a Rayleigh fluctuating target were studied, both with and without the presence of interfering targets. The single pulse analysis is extended here to a single pulse return from a Rayleigh-plus-dominant target. After demonstrating similar losses relative to a non-CFAR case, for either model of the fluctuations of the target, the analysis concentrates on a Rayleigh model which is easier to analyze analytically. A detailed analytic comparison between the performances of OS-CFAR, CA-CFAR [3], and censored CA-CFAR [4] is provided, for a Rayleigh target in the presence of strong interfering targets.

The analytic comparison between CA-CFAR and OS-CFAR is extended also to an integration of N pulses reflected from a Swerling II target. Here, the OS-CFAR performances (with and without interfering targets) yielded an integral equation which is solved numerically.

Thus, the performance comparison between OS-CFAR, CA-CFAR, and censored CA-CFAR is fully analytical, yielding either explicit expressions (for the single pulse case) or integral expressions (for the N pulses case). In that respect it differs from the comparison in [5] which resorts to Monte Carlo simulation methods.

The sensitivity of the CFAR property of OS to changes in the background statistics is also studied. An analytic expression of the false alarm probability of OS for a Weibull distributed background was derived. This provides a design formula for the correct threshold setting as function of the shape parameter C, as well as to an evaluation of the increase in P_{FA} as the Weibull shape parameter is reduced from an assumed Rayleigh value ($C = 2$) to lower values ($1.2 < C < 2$) that represent pdfs with a longer tail.

II. REVIEW OF NON-CFAR DETECTION

The pdfs of the amplitude of the fluctuating target are given by

$$p(A) = \frac{A}{A_0^2}\exp\left(-\frac{A^2}{2A_0^2}\right), \quad A \geq 0 \quad \text{(Rayleigh)} \tag{1}$$

$$p(A) = \frac{9A^3}{2A_0^4}\exp\left(-\frac{3A^2}{2A_0^2}\right), \quad A \geq 0 \quad \text{(Rayleigh + dominant)}. \tag{2}$$

With a noise (and clutter) rms of unit value, the average signal-to-noise ratio (SNR) is given by

$$\overline{\mathrm{SNR}} = A_0^2 \qquad \text{(Rayleigh)} \tag{3}$$

$$\overline{\mathrm{SNR}} = \frac{2}{3}A_0^2. \qquad \text{(Rayleigh + dominant)} \tag{4}$$

The pdf of z, the output of a square-law envelope detector, when the input is Rayleigh noise (and clutter) plus one of the two types of fluctuating targets, is given, respectively, by

$$p_1(z) = D\exp(-Dz) \qquad \text{(Rayleigh)} \tag{5}$$

where

$$D = \frac{1}{1+A_0^2} = \frac{1}{1+\overline{\mathrm{SNR}}} \tag{6}$$

and

$$p_2(z) = (1 + z - Gz)G^2\exp(-Gz) \qquad \text{(Rayleigh+dominant)} \tag{7}$$

where

$$G = \frac{3}{3+A_0^2} = \frac{2}{2+\overline{\mathrm{SNR}}}. \tag{8}$$

In the non-CFAR case, the probability of false alarm, for both cases, is a function of the (fixed) threshold Z_T

$$P_{\mathrm{FA}} = \int_{Z_T}^{\infty} p(z \mid A_0 = 0)\,dz = \exp(-Z_T). \tag{9}$$

The probabilities of detection are, respectively

$$P_{\mathrm{D}} = \exp(-DZ_T) \qquad \text{(Rayleigh)} \tag{10}$$

yielding

$$P_{\mathrm{D}} = (P_{\mathrm{FA}})^D \qquad \text{(Rayleigh)} \tag{11}$$

and

$$P_{\mathrm{D}} = [1 - (G^2 - G)Z_T]\exp(-GZ_T) \qquad \text{(Rayleigh+dominant)} \tag{12}$$

yielding

$$P_{\mathrm{D}} = [1 + (G^2 - G)\ln(P_{\mathrm{FA}})](P_{\mathrm{FA}})^G. \qquad \text{(Rayleigh+dominant)} \tag{13}$$

III. OS-CFAR

In OS-CFAR the inputs to M reference cells, after a square-law detector, are sorted in an increasing order, i.e.,

$$z_1 \le z_2 \le \cdots \le z_K \le \cdots \le z_M.$$

The threshold is obtained by selecting the Kth ranked cell to represent the noise and clutter level, and then multiplying the input to that cell by a scalar factor α. Thus the threshold

$$Z_T = \alpha z_K \tag{14}$$

is a random variable and its pdf is a function of the pdf of z_K [1]

$$p(z_K) = p_K(z) = K\binom{M}{K}[P(z)]^{K-1}[1 - P(z)]^{M-K}p(z) \tag{15}$$

where M is the number of reference cells, K is the rank of the representative cell, α is a scalar factor, $p(z)$ is the pdf of the inputs to the reference cells, and $P(z)$ is the distribution of the inputs to the reference cells.

For Rayleigh noise whose pdf and distribution are

$$p(z) = \exp(-z); \qquad P(z) = 1 - \exp(-z) \tag{16}$$

(15) becomes

$$p(z_K) = K\binom{M}{K}[1 - \exp(-z_K)]^{K-1} \times \exp[-z_K(M - K + 1)]. \tag{17}$$

The probability of detection is obtained by averaging the conditional probability of detection (given the threshold), over all possible values of the threshold. Thus

$$P_{\mathrm{D}} = \int_0^{\infty}\left[\int_{\alpha z_K}^{\infty} p_j(z)\,dz\right]p(z_K)\,dz_K, \qquad j = 1,2. \tag{18}$$

Choosing $j = 1$ selects the Rayleigh pdf (5). Choosing $j = 2$ selects the Rayleigh-plus-dominant pdf (7).

For the Rayleigh fluctuating target we obtain

$$P_{\mathrm{D}} = K\binom{M}{K}\int_0^{\infty}[1 - \exp(-z)]^{K-1} \times \exp[-z(M - K + 1 + \alpha D)]\,dz \tag{19}$$

which yields, [1],

$$P_{\mathrm{D}} = \frac{M!}{(M-K)!}\frac{\Gamma(\alpha D + M - K + 1)}{\Gamma(\alpha D + M + 1)} = \prod_{i=1}^{K}\left(1 + \frac{\alpha D}{M + 1 - i}\right)^{-1} \tag{20}$$

where $\Gamma(\ )$ is the Gamma function.

The probability of false alarm is obtained by setting $D = 1$ in (20)

$$P_{\mathrm{FA}} = \frac{M!}{(M-K)!}\frac{\Gamma(\alpha + M - K + 1)}{\Gamma(\alpha + M + 1)} = \prod_{i=1}^{K}\left(1 + \frac{\alpha}{M + 1 - i}\right)^{-1}. \tag{21}$$

Equation (21) allows us to obtain the factor α, for a given P_{FA}. Equations (6), (20), and (21) contain the triple relationship between P_{FA}, P_{D}, and the average SNR. An algorithm [2] involving the use of Sterling's formula, simplifies the numerical handling of this relationship.

For the Rayleigh-plus-dominant target, we use (7) in (18) and, after considerable manipulations, obtain

$$P_D = \frac{M!\Gamma(\gamma - K)}{(M-K)!\Gamma(\gamma)}\left\{1 + \alpha G(G-1)\left[\ln\left(1 - \frac{K}{\gamma}\right) - \frac{K}{2\gamma(\gamma - K)}\left(1 + \frac{2\gamma - K}{6\gamma(\gamma - K)}\right)\right]\right\} \quad (22)$$

where $\gamma \triangleq M + \alpha G + 1$.

Equation (22) together with (8) and (21) constitute the triple relationship for the Rayleigh-plus-dominant target.

A comparison between the two types of targets, for both OS-CFAR and non-CFAR processing, is presented in Fig. 1. The parameters are: $P_{FA} = 10^{-5}$, $M = 16$, and $K = 10$. We note an OS-CFAR loss of approximately 3 dB for both types of targets.

IV. MULTITARGET SITUATION

The presence of one or more interfering targets amongst the reference cells, causes the adaptive threshold to increase erroneously. In OS-CFAR this increase is relatively small. A reference cell with an input from a strong target will be ranked at the top, namely, it will occupy the Mth out of M cells. Thus the interfering target effectively reduces the number of reference cells to $M - 1$. The expected level of the input to the cell ranked K out of a total of $M - 1$ cells, will be only slightly higher than the level in the Kth ranked cell out of M cells. In the presence of J strong interfering targets, the effective number of reference cells drops to $M - J$. As was shown in [2], the detection loss due to the increase in threshold, is not extensive as long as $J \leq M - K$.

The effect of J interfering targets can be calculated using (22) after replacing in (22) M by $M - J$ and γ by $\gamma - J$. This yields a new relation between SNR (through G) and P_D. Note that α should still be calculated from (21) using M (and not $M - J$) and the nominal P_{FA}.

Fig. 2 summarizes the performances of OS-CFAR for a Rayleigh-plus-dominant target, with the parameters $P_{FA} = 10^{-5}$, $M = 16$, and $K = 10$, in the presence of $J = 0$, 2, and 4 interfering targets. Fig. 2 points to a loss of about 1 dB when two strong targets occupy two reference cells. Clearly this loss is an upper bound, and weaker interfering targets will cause a smaller loss.

The performance of OS-CFAR with a Rayleigh target and $J = 0$, 2, and 4 strong interfering targets, is presented in Fig. 3, indicating the same additional loss as in the Rayleigh-plus-dominant target. This limited comparison hints that the CFAR loss does not depend strongly on the target fluctuation model.

Rohling [1] pointed out that the choice of the order of the representative cell $-K$, effects slightly the performance of OS-CFAR without interfering targets. We present two more results with two other choices of K, and note their performance with and without interfering targets. Fig. 4 ($K = 12$) and Fig. 5 ($K = 14$), apply to a Rayleigh target and should be compared with Fig. 3 ($K = 10$). Note that for the case $J = 0$ (no interfering targets), performances improve slightly as K is increased. However, for $J = 2$, a choice of $K = 10$ or 12, yield almost identical results, while $K = 14$ yields an additional loss of about 1 dB. The reason for the poorer performances of $K = 14$ in the presence of $J = 2$ interfering targets stems from the fact that we reach the point in which $M - J = K$, implying that the representative cell becomes the highest ordered target-free reference cell. We conclude this chapter with a plot (Fig. 6) of OS-CFAR loss versus K, parametric in M, with no interfering targets.

V. COMPARISON WITH CA-CFAR AND CENSORED CA-CFAR

It is interesting to compare the effect of interfering targets on OS-CFAR with their effect on the basic CA-CFAR, which lacks inherent protection, and censored CA-CFAR [4] which (like OS-CFAR) can tolerate up to a predetermined number of interfering targets.

For the basic CA-CFAR processor it is necessary to define both the model and power of the interfering targets, relative to the power of the desired target. The detection probability of CA-CFAR in the presence of a *single* interfering target was analyzed in [3, 4].

For one or more interfering target, when both desired and interfering targets are Rayleigh distributed, and when all the interfering targets are independent, identically distributed (IID) (therefore have the same mean power), it was shown ([6, eqn. (18)] or [7, eqn. (21)]) that the probability of detection is given by

$$P_D = \left(\frac{\alpha D_1}{M D_2} + 1\right)^{-J}\left(\frac{\alpha D_1}{M} + 1\right)^{J-M}. \quad (23)$$

D_1 and D_2 are related to the average SNR of the desired and interfering targets, respectively, as defined in (6) and (3). M is the total number of reference cells, and J is the number of interfering targets. In CA-CFAR α is the scalar factor that multiplies the mean value of all the reference cells, in order to reach the threshold level. α is determined from the nominal P_{FA} by

$$\alpha = M\left(P_{FA}^{-1/M} - 1\right). \quad (24)$$

Note that setting $J = 1$ reduces (23) to [4, eqn. (7)].

Using (23), Fig. 7 displays the effect of $J = 0$, 1, 2, and 3 interfering targets on CA-CFAR, for the case when each interfering target has the same mean power

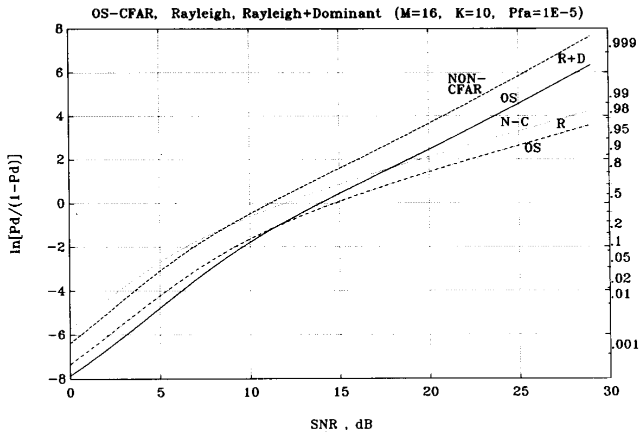

Fig. 1. Comparison between OS-CFAR and fixed-threshold detection for Rayleigh and Rayleigh + dominant targets.

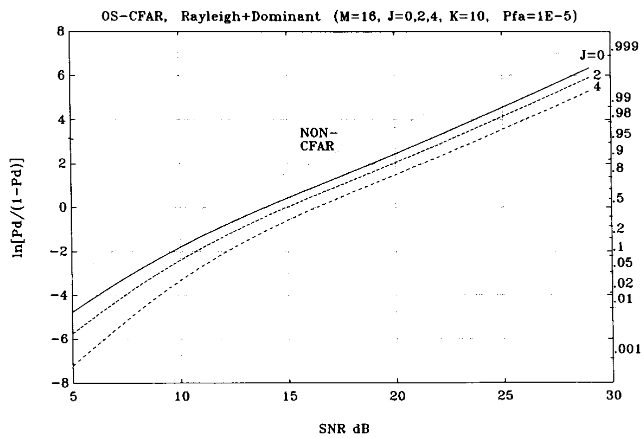

Fig. 2. Performances of OS-CFAR in detecting a Rayleigh + dominant target in presence of J strong interfering targets.

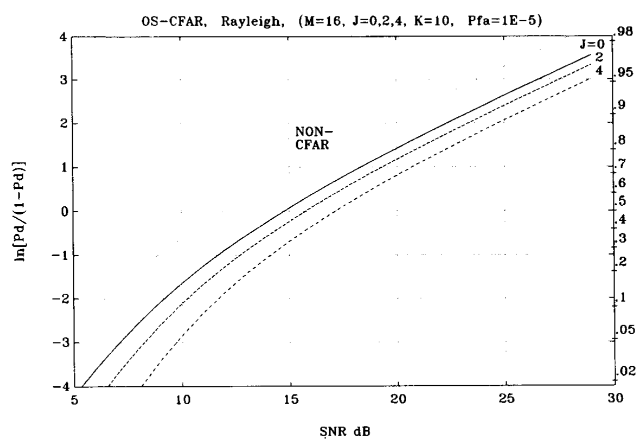

Fig. 3. Performances of OS-CFAR in detecting a Rayleigh target in presence of J strong interfering targets, when representative cell is 10th ranked out of 16 cells.

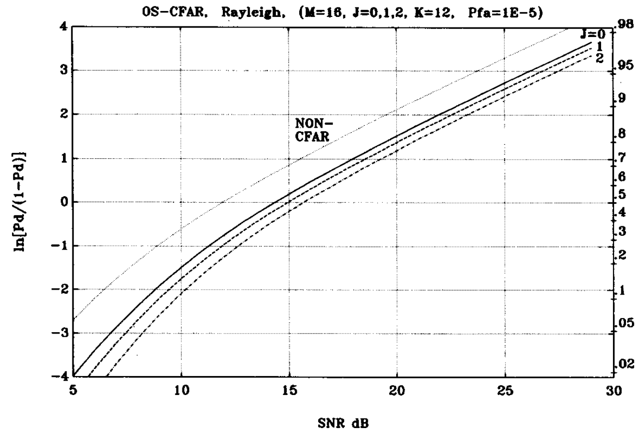

Fig. 4. Performances of OS-CFAR in detecting a Rayleigh target in presence of J strong interfering targets, when representative cell is 12th ranked out of 16 cells.

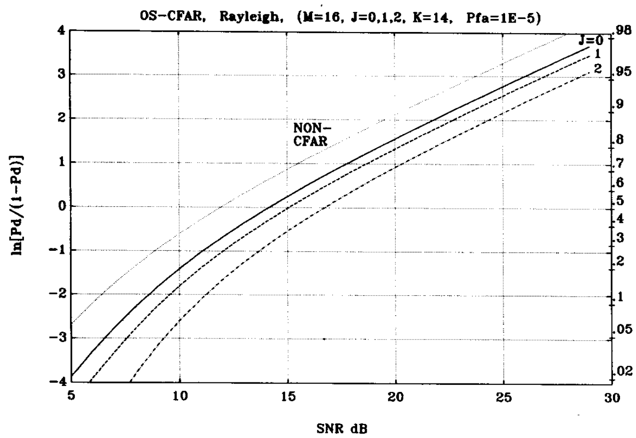

Fig. 5. Performances of OS-CFAR in detecting a Rayleigh target in presence of J strong interfering targets, when representative cell is 14th ranked out of 16 cells.

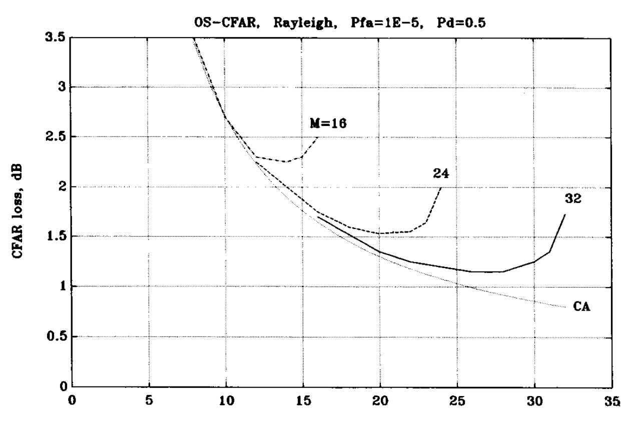

Fig. 6. Loss of OS-CFAR relative to fixed-threshold detector. ($P_{FA} = 10^{-5}$, $P_D = 0.5$.)

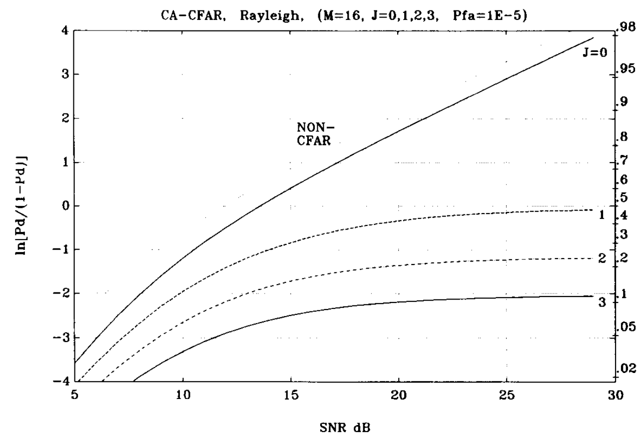

Fig. 7. Performances of CA-CFAR in detecting Rayleigh target in presence of J strong interfering targets.

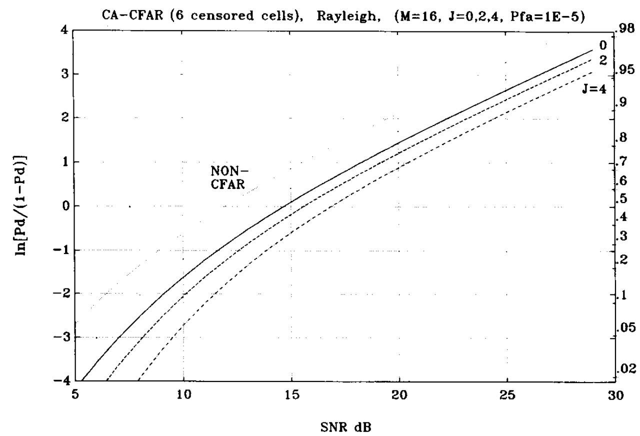

Fig. 8. Performances of CA-CFAR with 6 censored cells (out of 16) in presence of $J = 0, 2$ and 4 strong interfering targets.

as the desired target. Clearly the additional loss is very excessive. To overcome this problem, Rickard and Dillard [4] suggested the censored CA-CFAR.

Censored CA-CFAR [4] can be described as a hybrid between CA-CFAR and OS-CFAR. All the M reference cells are first ranked according to their magnitude, as in OS-CFAR. Next, the lowest K ranked cells are kept and averaged, as in CA-CFAR, and multiplied by a scalar factor to produce the threshold. A generalization of this concept, called trimmed-mean (TM) CFAR, was suggested in [7]. In TM-CFAR the lowest L ranked cells are also removed prior to averaging.

Ritcey [6] provided an analytic analysis of a censored mean level detector (CMLD), which differs slightly from the censored CA-CFAR. In the CMLD the threshold is determined from the lowest K samples of the ordered set $\{z_i\}$, by

$$Z_T = \alpha\left[(M-K)z_K + \sum_{i=1}^{K-1} z_i\right] \qquad (25)$$

where

$$\alpha = P_{FA}^{-1/K} - 1. \qquad (26)$$

Ritcey showed that in the presence of J strong interfering targets, the probability of detection of a Rayleigh target by the CMLD is given by

$$P_D = \binom{M-J}{K}\binom{M}{K}^{-1}\prod_{i=1}^{K}\left(1+\alpha D-\frac{J}{M+1-i}\right)^{-1}. \qquad (27)$$

The performance of a six-censored-cells CA-CFAR processor, which follows Ritcey's CMLD approach (with $M = 16$, $K = 10$, and $P_{FA} = 10^{-5}$) in the presence of $J = 0$, 2, and 4 strong interfering targets, are analyzed using (27) and presented in Fig. 8.

It is interesting to note that Fig. 8 is almost indistinguishable from Fig. 3 which represents the performances of an OS-CFAR with $K = 10$. Thus, this example and Fig. 6 demonstrate that when the highest uncensored rank of the CMLD-CFAR is equal to the representative rank of an OS-CFAR, both algorithms yield very similar performances.

VI. P_{FA} IN A WEIBULL BACKGROUND

The presence of strong targets in some of the reference cells represents one form of a deviation of the background statistics from the one which the CFAR processor was designed for. Another likely scenario is a homogeneous but different background statistics. Our analysis so far has assumed a Rayleigh distributed noise plus clutter. For such a background, a predetermined scalar factor α guaranties a constant false alarm rate. What happens when the background statistics deviates from Rayleigh? For CA-CFAR Goldstein [8] has shown a rapid increase of the P_{FA}, as the clutter pdf exhibits a longer tail typical of a log-normal pdf. Intuitively one would predict that OS-CFAR, which does not estimate the average background level, but the Kth ranking level, will have some more protection against unexpected long tailed pdfs, in particular, when the representative rank K is selected close to the highest rank $-M$.

In order to obtain a smooth transition from a Rayleigh background, we have extended the false alarm probability of OS-CFAR to cover the more general Weibull pdf, of which Rayleigh is a special case. The background clutter-plus-noise amplitude x will have a pdf,

$$p_5(x) = \frac{C}{B}\left(\frac{x}{B}\right)^{C-1} \exp\left[-\left(\frac{x}{B}\right)^C\right]. \qquad (28)$$

Note that by choosing the shape factor $C = 2$, the Weibull pdf reduces to the Rayleigh pdf (amplitude). It is well known that various clutter scenes fit a wider range of shape factors, usually within the limits $1.2 \leq C \leq 2$. A smaller shape factor implies a longer tailed pdf.

We should point out that the background is created by a vector sum of clutter and noise. The latter is usually Rayleigh distributed. By assuming a Weibull background we necessarily imply a large clutter-to-noise ratio.

When the OS processor follows a *square-law* detector, the inputs to the processor depend on x^2. Without loss of generality we can normalize with respect to B and obtain the normalized input random variable,

$$z = \left(\frac{x}{B}\right)^2 \qquad (29)$$

whose pdf is found from (28) to be

$$p_6(z) = \frac{C}{2} z^{(C/2)-1} \exp(-z^{C/2}) = -\left[\exp(-z^{C/2})\right]'. \qquad (30)$$

Integration of (30) yields the distribution function of z,

$$P_6(z) = 1 - \exp(-z^{C/2}). \qquad (31)$$

The pdf of the Kth ranked cell out of M cells, $p(z_k)$, is obtained by using (30) and (31) in (15), and the probability of false alarm is given by

$$P_{FA} = \int_0^\infty \left[\int_{\alpha z_K}^\infty p_6(z)\,dz\right] p(z_K)\,dz_K \qquad (32)$$

yielding

$$P_{FA} = \int_0^\infty \exp[-(\alpha z_K)^{C/2}] p(z_K)\,dz_K. \qquad (33)$$

Incorporating $p(z_K)$ in (33) we get

$$P_{FA} = \int_0^\infty \exp[-(\alpha z_K)^{C/2}] K \binom{M}{K} \left[1 - \exp(-z^{C/2})\right]^{K-1} \times \left[\exp(-z^{C/2})\right]^{M-K} \frac{C}{2} z^{(C/2)-1} \exp(-z^{C/2})\,dz. \qquad (34)$$

Solving (34) yields a simple result for the P_{FA} in a *Weibull* background,

$$P_{FA} = \frac{M!}{(M-K)!} \frac{\Gamma(\alpha^{C/2} + M - K + 1)}{\Gamma(\alpha^{C/2} + M + 1)} = \prod_{i=1}^{K} \left(1 + \frac{\alpha^{C/2}}{M + 1 - i}\right)^{-1}. \qquad (35)$$

The P_{FA} for a Weibull background clearly reduces to the P_{FA} for a Rayleigh background (21) when $C = 2$.

Equation (35) is an important result, providing us with the design formula for calculating the scalar factor α, for any desired P_{FA}, when the background is Weibull distributed, with a known shape parameter C.

An immediate example is the possibility to adopt Rohling's results, derived for a square-law detector, to a processor with a linear detector. A linear detector presents the processor with twice the shape parameter that a square-law detector presents. Hence, the scalar factor for a given P_{FA} has to be $\sqrt{\alpha}$, where α is the scalar factor that would have been calculated from (21) for the given P_{FA}.

Equation (35) also allows us to investigate the sensitivity of OS-CFAR to changes in the shape parameter of the background pdf. For example, if the OS-CFAR was designed assuming a Rayleigh background of clutter and noise, the scalar factor α had to be determined from (35) using $C = 2$ and the nominal P_{FA}. If now the actual background pdf had a longer tail, and could be fitted to a Weibull pdf with $C < 2$, the resulting P_{FA} can be easily calculated from (35) using the true shape parameter C.

Results of such an analysis, for a nominal $P_{FA} = 10^{-5}$ at $C = 2$, are presented in Fig. 9. The total number of reference cells is $M = 16$, and the rank K of the representative cell is the parameter. Fig. 9 clearly demonstrates that a higher choice of K yields a lower sensitivity of the P_{FA} to the shape parameter. Yet, even the highest possible K does not convert OS-CFAR to a two parameter CFAR processor, one which does not depend on both parameters (scale

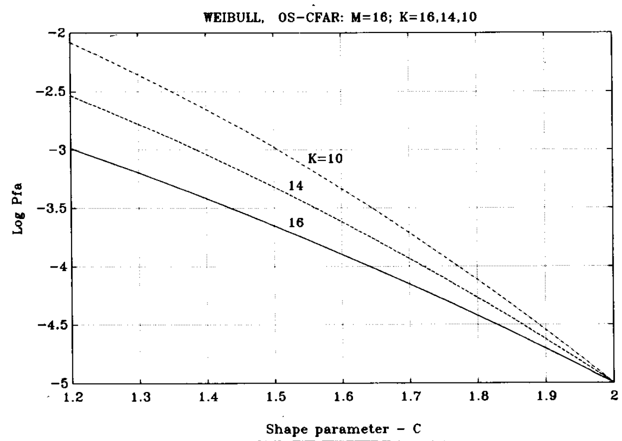

Fig. 9. False alarm probability of OS-CFAR in Weibull background as function of shape parameter C, when detector was designed for $P_{FA} = 10^{-5}$ at $C = 2$.

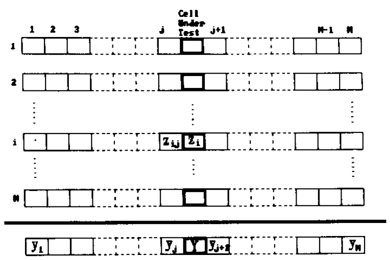

Fig. 10. Integration of N pulses in CFAR detector with M reference cells.

and shape) of a Weibull background pdf. Such a two-parameter OS-CFAR algorithm was suggested in [9]. It effectively estimates both the shape parameter and the scale parameter of a Weibull background, by using *two* ordered samples, instead of the one sample used in the original OS-CFAR algorithm. However, unless M is very large, the variance of the estimate of C is large, causing a considerable additional loss compared with the case of an a priori known C.

VII. OS-CFAR WITH NONCOHERENT INTEGRATION OF N PULSES

So far we have dealt with detection based on a single pulse. This chapter presents the performance analysis of OS-CFAR processing N pulses reflected from a Swerling II target. Recall that the magnitude of pulses reflected from a Swerling II target are IID random variables having a Rayleigh (amplitude) pdf. Swerling II targets were the only type which yielded a manageable OS-CFAR performance analysis, and even this analysis required numerical integration. The OS-CFAR performance is compared with CA-CFAR for which the probability of detection can be expressed in an explicit analytic formula. We show that for typical processor parameters, without interfering targets, the additional loss of OS-CFAR is less than 0.5 dB. When interfering targets are present, OS-CFAR maintains its inherent immunity.

The integrating CFAR processor is described in Fig. 10. A row represents the returns from one of the N pulses, while the columns to the left and to the right of the "cell under test" represent the M reference cells (e.g., range cells). We assume that the content of the reference cells (noise and clutter after a square-low detector) are IID random variables (RVs) z_{ij}, Rayleigh distributed with the pdf given in (16). A Swerling II target implies that the content of the cells in the column under test are also IID RVs with the pdf given in (5) and (6).

Integration of N pulses means that each column is added up. The sums appear in the bottom row. The RV describing the sum of the jth reference column is designated y_j, while the RV describing the sum of the column under test is designated Y.

The two new RVs created by the summation are

$$y_j = \sum_{i=1}^{N} z_{ij} \tag{36}$$

$$Y = \sum_{i=1}^{N} z_i. \tag{37}$$

Their corresponding pdfs are

$$p_3(y_j) = \frac{y_j^{N-1}}{(N-1)!} \exp(-y_j) \tag{38}$$

$$p_4(Y) = D^N \frac{Y^{N-1}}{(N-1)!} \exp(-DY) \tag{39}$$

where D is related to the average SNR as defined by (6).

A. CA-CFAR

In CA-CFAR the background estimate is obtained from the average of the M values of y_j. The first step in calculating the average is to obtain the sum

$$Y_S = \sum_{j=1}^{M} y_j = \sum_{j=1}^{M}\sum_{i=1}^{N} z_{ij}. \tag{40}$$

The pdf of Y_S is similar to the pdf of y_j, given in (38), but with N replaced by MN. The threshold is clearly $\alpha Y_S/M$, where α is the scalar factor used to adjust the probability of false alarm.

The probability of detection is obtained from

$$P_D = \int_0^\infty \left[\int_{\alpha Y_S/M}^\infty \frac{D^N Y^{N-1}}{(N-1)!}\exp(-DY)\,dY\right] \times \frac{Y_S^{MN-1}}{(MN-1)!}\exp(-Y_S)\,dY_S \tag{41}$$

which yields

$$P_D = \left(1+\frac{\alpha D}{M}\right)^{-MN}\sum_{j=0}^{N-1}\left(1+\frac{M}{\alpha D}\right)^{-j} \times \binom{MN-1+j}{j} \qquad \text{(CA-CFAR)} \tag{42}$$

where

$$D = \frac{1}{1+\text{SNR}}. \tag{43}$$

The probability of false alarm is obtained by setting $D = 1$ in (42)

$$P_{FA} = \left(1+\frac{\alpha}{M}\right)^{-MN}\sum_{j=0}^{N-1}\left(1+\frac{M}{\alpha}\right)^{-j} \times \binom{MN-1+j}{j}. \qquad \text{(CA-CFAR)} \tag{44}$$

Equation (44) is used to determine α from the desired P_{FA}.

The performances of CA-CFAR with noncoherent integration was studied by several authors, notably Mitchel and Walker [10]. Our results agree with [10] and are brought here in order to provide a comparison with OS-CFAR.

B. OS-CFAR

In OS-CFAR the background estimate is assumed to be the Kth ordered y_j, where $K \le M$. The threshold is again obtained from multiplying the background estimate by a scalar factor α. The pdf of the Kth ordered y_j is obtained by using (38) and its integral in (15). Thus,

$$p_K(y_K) = K\binom{M}{K}\left[\int_0^{y_K} p_3(y)\,dy\right]^{K-1} \times \left[1-\int_0^{y_K} p_3(y)\,dy\right]^{M-K} p_3(y_K). \tag{45}$$

The probability of detection is obtained from

$$P_D = \int_0^\infty \left[\int_{\alpha y_K}^\infty p_4(y)\,dy\right] p_K(y_K)\,dy_K. \tag{46}$$

Note that the integral of $p_3(y)$ is the incomplete gamma function which can be expressed as a finite sum. Namely,

$$\int_0^{y_K} \frac{y^{N-1}}{(N-1)!}\exp(-y)\,dy = 1-\exp(-y_K)\sum_{j=0}^{N-1}\frac{y_K^j}{j!}. \tag{47}$$

The integral of $p_4(y)$ is similarly obtained

$$\int_{\alpha y_K}^\infty \frac{D^N y^{N-1}}{(N-1)!}\exp(-Dy)\,dy = \exp(-\alpha D y_K)\sum_{j=0}^{N-1}\frac{(\alpha D y_K)^j}{j!}. \tag{48}$$

Using (45), (47), and (48) in (46) we get the probability of detection of OS-CFAR with integration of N pulses,

$$P_D = K\binom{M}{K}\int_0^\infty \left[\exp(-\alpha D y)\sum_{j=0}^{N-1}\frac{(\alpha D y)^j}{j!}\right] \times \left[1-\sum_{j=0}^{N-1}\frac{y^j\exp(-y)}{j!}\right]^{K-1}\left[\sum_{j=0}^{N-1}\frac{y^j\exp(-y)}{j!}\right]^{M-K} \times \frac{y^{N-1}\exp(-y)}{(N-1)!}\,dy. \tag{49}$$

Note that (49) reduces to (19) for $N = 1$.

Equation (49) has to be integrated numerically. The false alarm probability is obtained from (49) after setting $D = 1$. Numerical integration yields the relation between the desired P_{FA} and α. (several iterations are needed if the P_{FA} is given and α is the unknown). The numerical integration was performed over the boundaries $0 < y < 30$, using an integration step of $\Delta y = 0.1$.

Equations (42) and (49) are used to provide a specific comparison between CA-CFAR and OS-CFAR for a Swerling II target. The parameters used for this comparison are: $N = 10$ pulses, $M = 16$ reference cells, $P_{FA} = 10^{-5}$, and in the OS-CFAR case the representative rank is $K = 10$. The false alarm probability has yielded the scalar factors: $\alpha = 3.1472$ (CA-CFAR) and $\alpha = 3.1109$ (OS-CFAR).

The performances of both CFAR systems are presented in Fig. 11 together with the non-CFAR

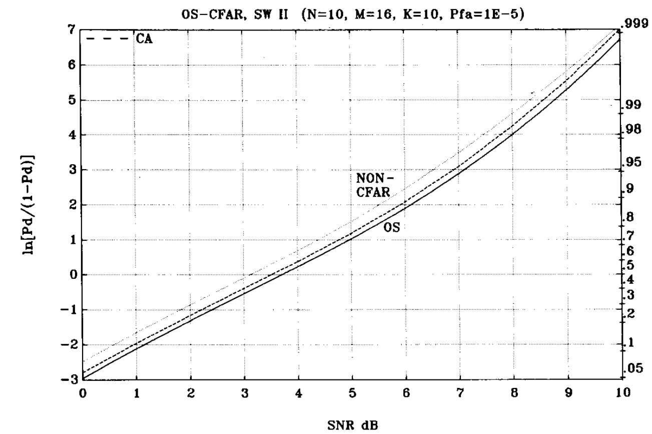

Fig. 11. Performances of fixed-threshold, CA-CFAR, and OS-CFAR detectors with integration of 10 pulses.

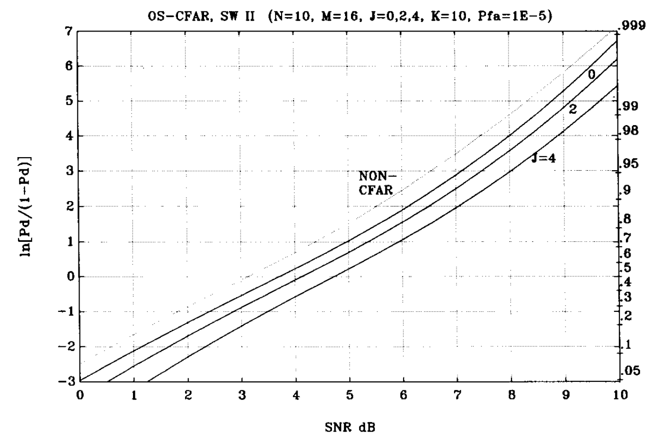

Fig. 12. Performances of OS-CFAR with integration of 10 pulses in presence of J strong interfering targets.

case. It is interesting to note that with integration of 10 pulses, the total loss of OS-CFAR is 0.65 dB, only 0.21 dB above the loss of CA-CFAR. The calculation was repeated for the case $M = 8$ and $K = 5$. Here, the total OS-CFAR loss was 1.18 dB, or 0.34 dB above CA-CFAR with $M = 8$ reference cells.

Integration does not deprive OS-CFAR from its inherent immunity to interfering targets. Its performance in the presence of J strong interfering targets among the reference cells, is again obtained by replacing M with $M - J$, when calculating P_D. (This requires the assumption that the cells occupied by the interfering targets do not change from pulse to pulse.) The results for $J = 0$, 2, and 4 interfering targets appear in Fig. 12.

REFERENCES

[1] Rohling, H. (1983)
Radar CFAR thresholding in clutter and multiple target situations.
IEEE Transactions on Aerospace and Electronic Systems, **AES-19** (July 1983), 608–621.

[2] Levanon, N. (1988)
Detection loss due to interfering targets in ordered statistics CFAR.
IEEE Transactions on Aerospace and Electronic Systems, **AES-24** (Nov. 1988), 678–681.

[3] Finn, H. M., and Johnson, R. S. (1968)
Adaptive detection mode with threshold control as a function of spatially sampled clutter-level estimates.
RCA Review, **29** (Sept. 1968), 414–464.

[4] Rickard, J. T., and Dillard, G. M. (1977)
Adaptive detection algorithms for multiple-target situations.
IEEE Transactions on Aerospace and Electronic Systems, **AES-13** (July 1977), 338–343.

[5] Barboy, B., Lomes, A., and Perkalsky, E. (1986)
Cell-averaging CFAR for multiple-target situations.
Proceedings of the IEE (London), **133**, Pt. F (Apr. 1986), 176–186.

[6] Ritcey, J. A. (1986)
Performance analysis of the censored mean-level detector.
IEEE Transactions on Aerospace and Electronic Systems, **AES-22** (July 1986), 443–454.

[7] Gandhi, P. P., and Kassam, S. A. (1988)
Analysis of CFAR processors in nonhomogeneous background.
IEEE Transactions on Aerospace and Electronic Systems, **AES-24** (July 1988), 427–445.

[8] Goldstein, G. B. (1973)
False-alarm regulation in log-normal and Weibull clutter.
IEEE Transactions on Aerospace and Electronic Systems, **AES-9** (Jan. 1973), 84–92.

[9] Weber, P., and Haykin, S. (1985)
Ordered statistics CFAR processing for two-parameter distributions with variable skewness.
IEEE Transactions on Aerospace and Electronic Systems, **AES-21** (Nov. 1985), 819–821.

[10] Mitchel R. L., and Walker, J. F. (1971)
Recursive methods for computing detection probabilities.
IEEE Transactions on Aerospace and Electronic Systems, **AES-7** (July 1971), 671–676.

Mordechai Shor was born in Israel in 1958. He received the B.Sc. and M.Sc. degrees in electrical engineering from Tel-Aviv University, Tel-Aviv, Israel, in 1980 and 1990, respectively.

Between 1980 and 1985 he served in the Israeli Army as an Electronic Engineer. Since then he has been with Tadiran System Division, Israel, working on COMINT systems.

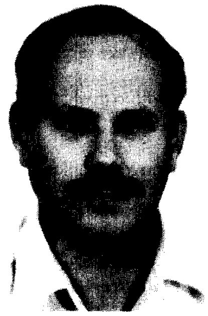

Nadav Levanon (S'67—M'69—SM'83) was born in Israel in 1940. He received the B.Sc. and M.Sc. in electrical engineering from the Technion-Israel Institute of Technology, Haifa, in 1961 and 1965, respectively, and the Ph.D. in electrical engineering from the University of Wisconsin, Madison, in 1969.

From 1961 to 1965 he served in the Israeli Army. He has been a faculty member at Tel-Aviv University since 1970, first in the Department of Geophysics, and since 1977 in the Department of Electronic Systems, where he is a Professor. He was Chairman of that department from 1983 to 1985. He was a Visiting Associate Professor at the University of Wisconsin, from 1972 to 1974, and a Visiting Scientist at The Johns Hopkins University, Applied Physics Laboratory, in the academic year 1982–1983.

He is the author of the book *Radar Principles* (Wiley, 1988).